

# Computational aspects of nuclear coupled-cluster theory

Gaute HAGEN<sup>1,2</sup> and Hai Ah NAM<sup>3</sup>

<sup>1</sup>*Department of Physics and Astronomy, University of Tennessee Knoxville, TN 37996, USA*

<sup>2</sup>*Physics Division, Oak Ridge National Laboratory, P.O. Box 2008, Oak Ridge, TN 37831, USA*

<sup>3</sup>*National Center for Computational Sciences Division, Oak Ridge Leadership Computing Facility, Oak Ridge National Laboratory, P.O. Box 2008, Oak Ridge, TN 37831, USA*

(Received March 16, 2012)

We discuss computational aspects of the spherical coupled-cluster method specific to the nuclear many-body problem. Using chiral nucleon-nucleon interaction at next-to-next-to-next-to leading order ( $N^3$ LO) with cutoff  $\Lambda = 500$ MeV, we present coupled-cluster results for the ground state of  $^{40}\text{Ca}$ . Scaling and performance studies are presented together with challenges we meet with when extending the coupled-cluster effort to nuclei mass hundred and beyond.

## §1. Introduction

The low-energy nuclear many-body problem is a challenging undertaking, however, in the last decade there has been significant progress in first principle calculations of nuclei.<sup>1),2),3),4),5),6),7),8),9)</sup> With the advance of chiral effective field theory<sup>10),11),12),13),14),15)</sup> which allows for a systematic and consistent derivation of the nuclear forces rooted in low-energy Quantum-Chromo-Dynamics (QCD), and with the development of advanced many-body methods and high performance computing facilities, first principle computations of medium mass and neutron rich nuclei at the extremes of the nuclear chart are now within reach. The computational cost involved in these calculations grows rapidly as one moves beyond the lightest towards the medium mass region and beyond, and it has been crucial to implement techniques that scale gently with system size and code development that leverages the benefits of modern architecture at high-performance computing facilities.

The coupled-cluster (CC) method is an optimal approach to medium mass and neutron rich nuclei as it is an ideal compromise between accuracy on the one hand and computational cost on the other. Coupled-cluster theory was introduced in nuclear physics in the late 1950's by Coester and Kümmel<sup>16),17)</sup> and was shortly thereafter introduced in quantum chemistry by Čížek.<sup>18),19)</sup> Coupled-cluster theory has now been established as the “gold standard” for first principle computations in quantum chemistry, see Ref.<sup>20)</sup> for a recent review. Only in the last decade has coupled-cluster reemerged in the nuclear physics community and has established itself as a state-of-the art approach to structure of medium mass and neutron rich nuclei.<sup>21),22),23),24),25),26),27),28)</sup>

The nuclear coupled-cluster code suite developed at Oak Ridge National Laboratory, called NUCCOR (Nuclear Coupled-Cluster - Oak Ridge) has been further advanced under UNEDF (Universal Nuclear Energy Density Functional) a five-year SciDAC (Scientific Discovery through Advanced Computing) project.<sup>29),30)</sup> Both  $m$ -scheme (NUCCOR) and  $j$ -coupled (spherical) (NUCCOR-CCSD(T)) schemes for implementing CC at various levels of clustering approximation (i.e. single, doubles, triples, etc.) has been developed. Under UNEDF, considerable effort has been put into optimizing the NUCCOR-CCSD(T) V1.0 doubles kernel for the Jaguar Cray XT5 system, Oak Ridge Leadership Computing Facility's (OLCF) flagship leadership computing resource.<sup>31)</sup>

To continue to achieve breakthrough discoveries in low-energy nuclear physics using CC, we need to push investigations to larger medium-mass nuclei in larger model spaces. This requires continued emphasis on scaling the CC algorithms and performance optimization. Additionally, Jaguar is presently undergoing a multi-phase upgrade to become Titan, a Cray XK6 with a single socket of AMD's 16-core interlagos chip with 32 GB of shared memory and another socket with the NVidia GPUs on a single node. Therefore we need to further develop and improve our implementation of coupled-cluster theory in preparation for the architectural change.

This paper is organized as follows. In section 2 we provide an overview of the spherical coupled-cluster method used in NUCCOR-CCSD(T) and present convergence properties for the ground state of  $^{40}\text{Ca}$ . Section 3 describes the computational considerations of the CC code suite and presents performance results on Jaguar XK6 without GPUs, and describes future code developments necessary for continued research. Section 4 provides conclusions and outlook.

## §2. Nuclear coupled-cluster theory

In coupled-cluster theory we write the  $A$ -nucleon ground state wave function  $|\Psi_0\rangle$  in the following form

$$|\Psi_0\rangle = e^{-\hat{T}}|\phi_0\rangle, \quad \hat{T} = \hat{T}_1 + \hat{T}_2 + \dots + \hat{T}_A. \quad (2.1)$$

Here  $|\phi_0\rangle$  is the uncorrelated (mean-field) reference state, and  $\hat{T}$  is a linear expansion in particle-hole excitations operators. The  $k$ -particle  $k$ -hole ( $k$ p- $k$ h) cluster operator is

$$\hat{T}_k = \frac{1}{(k!)^2} \sum_{i_1, \dots, i_k; a_1, \dots, a_k} t_{i_1 \dots i_k}^{a_1 \dots a_k} \hat{a}_{a_1}^\dagger \dots \hat{a}_{a_k}^\dagger \hat{a}_{i_k} \dots \hat{a}_{i_1}. \quad (2.2)$$

Here and in the following,  $i, j, k, \dots$  label occupied single-particle orbitals while  $a, b, c, \dots$  label unoccupied orbitals. From the exponential wave-function ansatz in Eq. (2.1) it follows directly that coupled-cluster theory is based on the similarity transform

$$\overline{H}_N = e^{-\hat{T}} \hat{H}_N e^{\hat{T}} \quad (2.3)$$

of the normal-ordered Hamiltonian  $\hat{H}_N$ . Here, the Hamiltonian is normal-ordered with respect to a reference state  $|\phi_0\rangle$ . The most commonly used approximation is coupled-cluster with singles-and-doubles excitations (CCSD) where  $\hat{T} \approx \hat{T}_1 + \hat{T}_2$ .

The unknown amplitudes  $t_i^a$  and  $t_{ij}^{ab}$  in Eq. (2.2) are determined from the solution of the coupled-cluster equations

$$0 = \langle \phi_i^a | \bar{H} | \phi_0 \rangle, \quad (2.4)$$

$$0 = \langle \phi_{ij}^{ab} | \bar{H} | \phi_0 \rangle. \quad (2.5)$$

Here  $|\phi_i^a\rangle = \hat{a}_a^\dagger \hat{a}_i |\phi_0\rangle$  is a 1p-1h excitation of the reference state, and  $|\phi_{ij}^{ab}\rangle$  is a similarly defined 2p-2h excited state. The CCSD equations (2.4) thus demand that the reference state  $|\phi_0\rangle$  has no 1p-1h and no 2p-2h excitations, i.e. it is an eigenstate of the similarity transformed Hamiltonian (2.3) in the space of all 1p-1h and 2p-2h excited states. Once the CCSD equations are solved, the ground-state energy is computed as

$$E = \langle \phi_0 | \bar{H} | \phi_0 \rangle. \quad (2.6)$$

Using Wick's theorem the coupled-cluster equations in (2.4) can be written as a set of coupled non-linear set of equations in the  $t_i^a$  and  $t_{ij}^{ab}$  amplitudes. However, this task is very tedious and error prone, and a much more direct and intuitive derivation proceeds via a diagrammatic derivation using a set of well defined diagram rules (see e.g. Ref.<sup>20</sup>). In the CCSD approximation the number of non-linear equations are given by  $n_o n_u + n_o^2 n_u^2$ . Here  $n_o$  is the number of occupied orbitals in the reference state and  $n_u$  is the number of unoccupied states above the fermi level. In a typical case calculating the CCSD ground state of <sup>40</sup>Ca in 15 major oscillator shells we have a total of 40 occupied and 2680 unoccupied orbitals, resulting in a total of  $\sim 10^{10}$  non-linear coupled equations. This problem is too large to be solved by direct inversion techniques, and we use an iterative solution scheme together with krylov subspace methods such as Broyden<sup>32),33)</sup> or Direct-Inversion in the Iterative Sub-Space (DIIS)<sup>34)</sup> as convergence accelerators.

The most expensive contribution to the  $T_2$  amplitude in the CCSD approximation is

$$t_{ij}^{ab} \leftarrow \sum_{cd} \langle ab | \chi | cd \rangle t_{ij}^{cd}, \quad (2.7)$$

it is clear that the computational cost associated with this contribution is  $n_o^2 n_u^4$ . Coupled-cluster theory therefore scales polynomial with the system size, which is a rather soft scaling compared to the combinatorial scaling of methods such as the full configuration interaction (FCI) method. Equation (2.7) can be rewritten in a matrix-matrix multiplication form, so that we can utilize the optimized basic linear algebra library (BLAS).<sup>35)</sup> Although the scaling of the CC method is rather soft, it is clear that due to memory limitations we quickly reach the limit of the maximum model space that can be handled on modern computers. For example, in 15 major oscillator shells the two-body interaction alone would require about 600 TByte of memory alone and the  $T_2$  amplitudes would require 100 GByte of memory.

In order to overcome this bottleneck, we recently derived and implemented the coupled-cluster equations in a coupled-angular momentum scheme,<sup>25),8)</sup> thereby utilizing the spherical symmetry of closed shell nuclei. For such nuclei, the cluster operator in Eq. (2.2) is a scalar under rotation, and depends only on reduced amplitudes. The reduced matrix elements of the Hamiltonian are stored in six different

blocks according to

$$[pppp], [hppp], [hhpp], [hphp], [hhhp], [hhhh],$$

where  $p$  denotes particle states and  $h$  denotes hole states. These matrices are sparse and block diagonal, each block is defined by a set of quantum numbers  $J^\pi, T_z$ . The largest matrices are the  $[pppp]$  and  $[hppp]$  are distributed among the processors by adding row by row to given processor until a criterion for optimal load balancing and memory distribution is reached, as illustrated in Fig. 1 By this distribution scheme

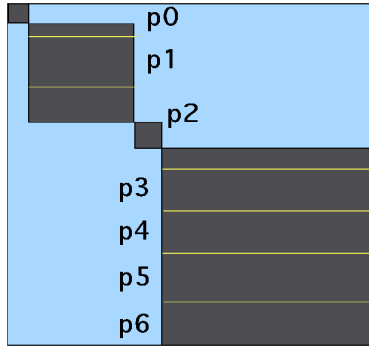


Fig. 1. (Color online) Block diagonal structure of the interaction and parallel distribution scheme

each processor will have a set of square and rectangular matrices for a subset of channels (quantum numbers)  $J^\pi, T_z$ . By this scheme, we can utilize the optimized linear algebra libraries Blas and Lapack<sup>35)</sup> for matrix-matrix and matrix-vector operations. It is clear that the similarity transformed Hamiltonian is also a scalar under rotation and can be distributed in the same scheme, and it is straight forward (but somewhat tedious) to work out the CCSD equations within this formulation.

As an example of the computational savings we achieve by switching from an uncoupled to a  $j$ -coupled scheme, we consider the case of  $^{40}\text{Ca}$  in 15 major shells. In  $m$ -scheme we have a total of 2720 orbitals while in the coupled  $j$ -scheme we have 240 orbitals, the number of non-linear CCSD equations in  $m$ -scheme is  $\sim 10^{10}$  while in  $j$ -scheme we have  $\sim 10^6$ . The various interaction blocks in Fig. 2 appear in various topologically different diagrams in the CCSD equations. Therefore it is very difficult to make the CCSD code scale optimally with increasing number of processors. We choose to distribute the blocks according to the number of computational cycles of the most expensive diagrams they appear in. Therefore scaling can only be optimal for these subsets of diagrams, while the remaining ones will scale less optimally.

To illustrate the convergence properties of the coupled-cluster ground state as a function of model space size we compute the ground state of  $^{40}\text{Ca}$  within  $\Lambda$ -CCSD(T) approach.<sup>8)</sup> We start from the intrinsic Hamiltonian where the nucleon-nucleon interaction is given by the  $N^3\text{LO}$  interaction ( $A_\chi = 500 \text{ MeV}c^{-1}$ ) by Entem and Machleidt.<sup>15),13)</sup> The nucleon-nucleon interaction is given in relative coordinates, and in order to express it in a harmonic oscillator single-particle basis we need to transform it to the laboratory frame using the Brody-Moshinsky transformation.<sup>36)</sup>

This transformation depends on the number of partial waves we include in the relative coordinate frame given, and is given by  $J_{\text{rel-max}}$ . In order to have fully converged calculations we need to make sure we have included sufficient number of partial waves in the Brody-Moshinsky transformation. The convergence is therefore two-fold, (i) as a function of the single-particle basis size, and (ii) as a function of number of relative partial waves included in the relative-to-laboratory frame transformation. We perform our calculations using a Hartree-Fock basis expressed in a harmonic oscillator single-particle basis with a frequency of  $\hbar\omega = 26$  MeV. In Fig. 2 we show the convergence for the ground state of  $^{40}\text{Ca}$  as a function of number of harmonic oscillator shells  $N = 2n + l$  (left figure), and as a function of  $J_{\text{rel-max}}$  for the Brody-Moshinsky transformation, keeping the single-particle space fixed at  $N = 16$  shells (right figure). We see that  $N = 16$  is sufficient size for the single-particle model space in order to converge the ground state to within 1 MeV, while we need to include relative partial waves up to  $J_{\text{rel-max}} = 8, 10$  to reach convergence for the Brody-Moshinsky transformation. In our earlier calculations<sup>25),8)</sup> we used  $J_{\text{rel-max}} = 4$ , and therefore underestimated the binding energy of  $^{40}\text{Ca}$  by  $\sim 15$  MeV.

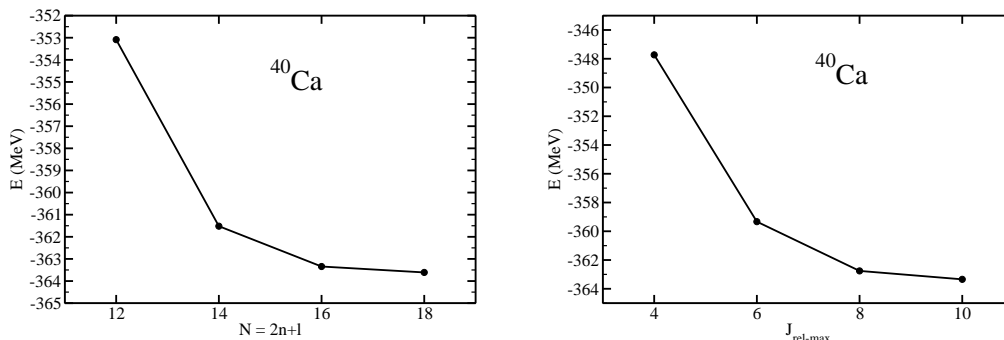


Fig. 2. Convergence of  $\Lambda$ -CCSD(T) ground state energy of  $^{40}\text{Ca}$  as a function  $N = 2n + l$  (left figure) and  $J_{\text{rel-max}}$  (right figure)

### §3. Computational Considerations

In coupled-cluster calculations, the computational challenge consists of scaling the computational resources with the increasing size of the model space and size of nuclei. For an interaction with momentum cutoff  $\Lambda$  and a nucleus with radius  $R$ , the size of the single-particle basis scales as  $(R\Lambda)^3 \sim A\Lambda^3$ ,<sup>8)</sup> with  $A$  being the mass number. In 20 oscillator shells, the matrix elements of the two body-interaction require about 100 GByte of memory, and for tin isotopes, we expect that 25-30 shells will be required for present-day chiral interactions.

The NUCCOR-CCSD(T) application has been developed for the Jaguar super-computer located at Oak Ridge National Laboratory. It utilizes MPI and threaded BLAS and LAPACK libraries, suited for the Cray XT5 architecture comprised of

dual hex-core processors with 16 GB of memory on the node. Jaguar is presently undergoing a phased upgrade from an XT5 to an eventual Cray XK6, called Titan, with a single interlagos 16-core chip with 32 GB of memory paired with NVidia GPUs. The current phase of the upgrade has fully deployed the CPU enhancements with the GPU additions expected to complete at the end of 2012.

Hybrid programming, using both MPI and OpenMP, is more advantageous in the current configuration of the system due to the large shared memory and the large number of cores on a single node. In an effort to efficiently utilize this new architecture, we have made added further parallelism in the triples calculation using OpenMP. This section presents performance results of the improved NUCCOR-CCSD(T) V2.0 application on the current Jaguar XK6 configuration, without GPUs.

### 3.1. Scaling by model space

Figure 3 shows strong scaling results for NUCCOR-CCSD(T) V2.0 using the PGI 11.10.0 compiler with optimization *-fast* and the Cray LibSci 11.0.4 scientific threaded library for  $^{40}\text{Ca}$  in model spaces  $N = 12, 14, 16$  and  $18$ . Runtimes for the triples calculation are presented with total runtimes along with labels showing the percentage of runtime used in the triples calculation at various numbers of cores. These calculations utilize 4 MPI processes each spawning 4 threads using OpenMP and the threaded libraries to optimally use all cores on a node.

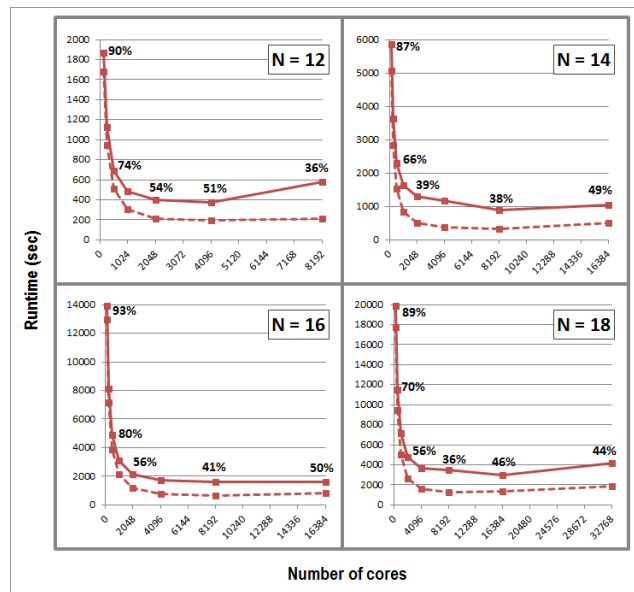


Fig. 3. (Color online) Strong scaling results for  $^{40}\text{Ca}$  in model spaces  $N = 12$ ,  $N = 14$ ,  $N = 16$ , and  $N = 18$ . Dashed lines show triples runtime only and solid lines represent total runtime. Percentage labels show percent of total runtime spent in triples calculation.

Seen in all model spaces, the runtime of NUCCOR-CCSD(T) V2.0 is dominated by the triples calculation at small numbers of processors, consuming roughly 90% of the total runtime. Utilizing more processors shows a dramatic decrease in the runtime of the triples calculation, which in turn decreases the overall runtime. At

larger numbers of processors, the triples calculation consumes less than 50% of the total runtime, indicating a necessity to revisit performance optimizations for other regions of the code, including the single and doubles calculation, setup, and I/O, which consume the remainder of the runtime.

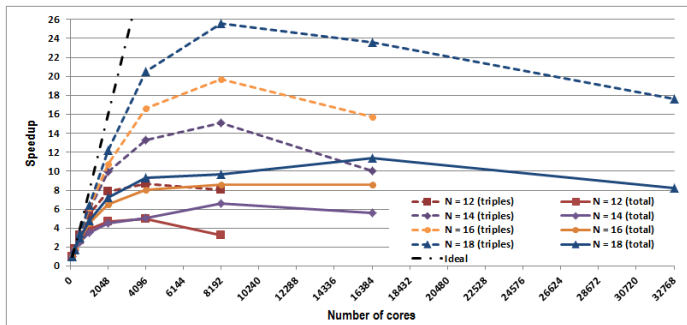


Fig. 4. (Color online) Speedup from 8 nodes (128 cores) for  $^{40}\text{Ca}$  in model spaces  $N = 12$  (red square),  $N = 14$  (purple diamond),  $N = 16$  (orange circle), and  $N = 18$  (blue triangle). Dashed lines show triples runtime only and solid lines represent total runtime.

The highest number of cores used in each model space shows the limits of strong scaling for both the triples and the total runtime. This is further evident in the speedup trends shown in Fig. 4, where the speedup at each model space drops sharply at the highest processor count for each model space. We use 128 cores for  $T(1)$  in the speedup calculations, which is the smallest configuration to run all model spaces. Figure 4 shows drastic speedup in the triples calculations with larger number of cores, but that the total runtime only improves by roughly half those values. With improvements in the triples calculation, which originally dominated the NUCCOR-CCSD(T) runtime, other regions of code utilizing MPI only will also require further parallelization to utilize the new architecture.

### 3.1.1. MPI vs. Threading

Although the use of threads through OpenMP has greatly improved the triples calculation and thus the overall runtime, Fig. 5 shows that increasing the number of threads does not improve the total runtime. In Fig. 5 we present scaling results using three configurations, varying the number of MPI processes and threads per process. We show that using 4 MPI processes and 4 threads performs equally well for the triples calculation as using 2 MPI processes and 8 threads. Due to the MPI only regions of code, yet to be optimized for the new architecture, the total runtime is worse using less MPI processes and more threads. Also shown in Fig. 5 is a degradation in performance when using more MPI processes and less threads (8 MPI process and 2 threads) since it does not allow the benefits of threading to be realized.

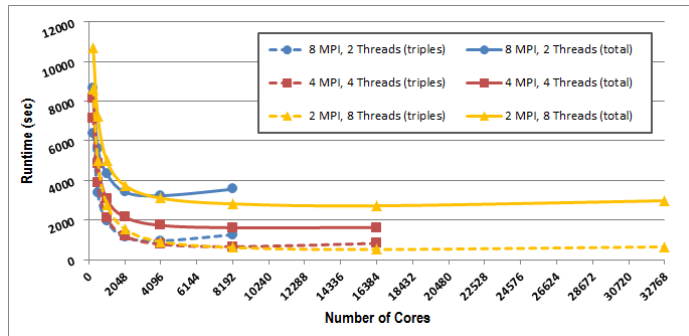


Fig. 5. (Color online) Comparison of runtimes (in seconds) of NUCCOR-CCSD(T) V2.0 for  $^{40}\text{Ca}$ ,  $N = 16$  with varying MPI processes and threads. Dashed lines show triples runtime only and solid lines represent total runtime. Thread configurations include: 8 MPI processes with 2 threads each (blue dot), 4 MPI processes with 4 threads each (red square), and 2 MPI processes with 8 threads each (yellow triangle) on a node. All compute cores on the node are utilized.

#### §4. Conclusions and future perspectives

We have made substantial performance improvements in NUCCOR-CCSD(T) V2.0 by implementing threading in the triples calculation using OpenMP. For example, our triples calculation consumed 70 – 95% of the runtime, scaling to 8192 cores for  $N=18$  in  $^{40}\text{Ca}$ . This example used 4 MPI processes each spawning 4 threads, resulting in a total number of 32768 requested MPI processes. Note that we typically need several runs of this size for each nucleus, in order to determine convergence and to map out the dependence on the model space parameters.

These improvements now reveal new areas for continued development to optimize the total runtime performance to reach nuclei larger than  $^{40}\text{Ca}$  in larger model spaces. Improvements include further threading MPI only regions, including the singles and doubles calculations, setup, and improvements to I/O.

In preparation for utilizing the full capability of Titan, the hybrid CPU-GPU system, which will be available in Q4 of 2012, we are also going through the exercise of identifying compute-intensive kernels suitable to be off-loaded to the GPU and implementing GPU-optimized libraries, GPU directives, and GPU languages such as CUDA and OpenCL, as needed to continue to improve the models and implement more realistic system constraints. For example, the inclusion of continuum effects in weakly bound nuclei and nuclear reactions will require us to utilize a large number of scattering states which further increases the size of the model space. Increasing the order of the coupled-cluster approximation and including higher-body effects, such as three-body and four-body forces, present additional computational challenges to both developers and computing systems.

#### §5. Acknowledgments

This work was supported by the Office of Nuclear Physics, U.S. Department of Energy (Oak Ridge National Laboratory). This work was supported in part by



the U.S. Department of Energy under Grant No. DE-FC02-07ER41457 (UNEDF SciDAC). This research used resources of the National Center for Computational Sciences at Oak Ridge National Laboratory, which is supported by the Office of Science of the U.S. Department of Energy under Contract No. DE-AC05-00OR22725.

### References

- 1) S. C. Pieper and R. B. Wiringa, *Ann. Rev. Nucl. Part. Sci.* **51**, 53 (2001).
- 2) P. Navratil, S. Quaglioni, I. Stetcu and B. R. Barrett, *J. Phys. G: Nucl. Part. Phys.* **36**, 083101 (2009).
- 3) E. Epelbaum, H. Krebs, D. Lee, and U.-G. Meißner *Phys. Rev. Lett.* **104**, 142501 (2010).
- 4) K. Tsukiyama, S. K. Bogner, and A. Schwenk, *Phys. Rev. Lett.* **106**, 222502 (2011).
- 5) R. Roth, *Phys. Rev. C* **79**, 064324 (2009).
- 6) C. Barbieri, *Phys. Rev. Lett.* **103**, 202502 (2009).
- 7) S. Fujii, R. Okamoto, and K. Suzuki, *Phys. Rev. Lett.* **103**, 182501 (2009).
- 8) G. Hagen, T. Papenbrock, D. J. Dean, and M. Hjorth-Jensen *Phys. Rev. C* **82**, 034330 (2010).
- 9) P. Maris, J. P. Vary, and A. M. Shirokov, *Phys. Rev. C* **79**, 014308 (2009).
- 10) S. Weinberg, *Phys. Lett. B* **251**, 288 (1990); *Nucl. Phys. B* **363**, 3 (1991).
- 11) U. van Kolck, *Phys. Rev. C* **49**, 2932 (1994).
- 12) E. Epelbaum, W. Glöckle, and U. G. Meißner, *Nucl. Phys. A* **671**, 295 (2000).
- 13) D. R. Entem and R. Machleidt, *Phys. Rev. C* **68**, 041001(R) (2003).
- 14) E. Epelbaum, W. Glöckle, and U. G. Meißner, *Nucl. Phys. A* **747**, 362 (2005).
- 15) D. R. Entem and R. Machleidt, *Phys. Lett.* **B524**, 93 (2002).
- 16) F. Coester, *Nucl. Phys.* **7**, 421 (1958).
- 17) F. Coester and H. Kümmel, *Nucl. Phys.* **17**, 477 (1960).
- 18) J. Čížek, *J. Chem. Phys.* **45**, 4256 (1966).
- 19) J. Čížek, *Adv. Chem. Phys.* **14**, 35 (1969).
- 20) R.J. Bartlett and M. Musiał, *Rev. Mod. Phys.* **79**, 291 (2007).
- 21) J.H. Heisenberg and B. Mihaila, *Phys. Rev. C* **59**, 1440 (1999).
- 22) B. Mihaila and J.H. Heisenberg, *Phys. Rev. C* **61**, 054309 (2000); *Phys. Rev. Lett.* **84**, 1403 (2000).
- 23) D.J. Dean and M. Hjorth-Jensen, *Phys. Rev. C* **69**, 054320 (2004).
- 24) K. Kowalski, D.J. Dean, M. Hjorth-Jensen, T. Papenbrock, and P. Piecuch, *Phys. Rev. Lett.* **92**, 132501 (2004).
- 25) G. Hagen, T. Papenbrock, D. J. Dean, and M. Hjorth-Jensen, *Phys. Rev. Lett.* **101**, 092502 (2008).
- 26) G. R. Jansen, M. Hjorth-Jensen, G. Hagen, T. Papenbrock, *Phys. Rev. C* **83**, 054306 (2011).
- 27) G. Hagen, T. Papenbrock, M. Hjorth-Jensen, *Phys. Rev. Lett.* **104**, 182501 (2010).
- 28) R. Roth, S. Binder, K. Vobig, A. Calci, J. Langhammer, P. Navratil, <http://arxiv.org/abs/1112.0287v1> (2012).
- 29) G. F. Bertsch, D. J. Dean and W. Nazarewicz *SciDAC Review* **6** 42 (2007).
- 30) R. J. Furnstahl (for the UNEDF Council) *Nuclear Physics News* **21** 18 (2011).
- 31) W. Joubert, D. Kothe and H. Nam *Preparing for Exascale: ORNL Leadership Computing Facility Application Requirements and Strategy* (Oak Ridge: ORNL) (2009).
- 32) D. D. Johnson, *Phys. Rev. B* **38**, 12807 (1988).
- 33) A. Baran, A. Bulgac, M. M. Forbes, G. Hagen, W. Nazarewicz, N. Schunck, and M. V. Stoitsov, *Phys. Rev. C* **78**, 014318 (2008).
- 34) P. Pulay, *Chem. Phys. Lett.* **73**, 393 (1980).
- 35) For a full documentation of the B(asic)L(inear)A(lgebra)S(ubprograms) software, see [urlhttp://www.netlib.org/blas](http://www.netlib.org/blas).
- 36) T. A. Brody, M. Moshinsky, *Tables of Transformation Brackets*, Monografias del Instituto de Fisica, Universidad Nacional Autonoma de Mexico, 1960.